Journal of
Low Power Electronics and Applications

MDPI

Article

An Empirical Method for Predicting the Critical Current of Unshunted Josephson Junctions in a Shielded Room from Measurements in an Unshielded Room

Jian Zhou [1,*], Juan Wang [2], Yewen Yao [2], Yongliang Wang [1], Man Wang [2] and Wei Peng [1]

[1] Shanghai Institute of Microsystem and Information Technology (SIMIT), Chinese Academy of Sciences (CAS), Shanghai 200050, China; wangyl@mail.sim.ac.cn (Y.W.); wpeng@mail.sim.ac.cn (W.P.)
[2] School of Computer and Information Engineering, Shanghai Polytechnic University, Shanghai 201209, China; 20211510151@stu.sspu.edu.cn (J.W.); yaoyewen@hsic.cn (Y.Y.); wangman@sspu.edu.cn (M.W.)
* Correspondence: zjian@mail.sim.ac.cn

Abstract

The critical current (I_c) of a Josephson junction (JJ) is a significant physical parameter that plays a crucial role in the design of subsequent devices and circuits, as well as in the optimization of manufacturing processes. To ensure accurate measurements, testing should ideally be conducted in a magnetically shielded room. However, due to laboratory constraints, tests are often performed in unshielded environments, where they are inevitably influenced by various environmental noises. This introduces significant uncertainty into the measured I_c values, thereby impacting the design of subsequent superconducting circuits. This study examines the impact of conductive, radiated, and flux noise on the repeatability of I_c measurements in an unshielded environment and establishes an empirical formula for predicting I_c values in shielded environments based on unshielded data. The deviation between the empirically predicted I_c and the experimentally measured value is less than 1%, verifying the effectiveness of the proposed formula. This approach offers a relatively accurate and cost-effective method for testing the critical current (I_c) of Josephson junctions (JJs) under unshielded conditions.

Keywords: unshunted Josephson junctions; measurement; critical current; formula; uncertainty

1. Introduction

Superconducting electronic circuit technology is characterized by high clock frequencies [1] and minimal bit manipulation energy dissipation [2,3], making it a promising candidate for future high-performance superconducting computers. The MIT Lincoln Laboratory (MIT LL) has achieved significant advancements in the manufacturing technology of superconducting rapid single flux quantum (RSFQ) circuits [4–7]. These circuits are designed for high-performance superconducting multi-bit processors with clock frequencies ranging from 10 GHz to 20 GHz [8–12]. Conventional processes typically employ shunted Josephson junctions (JJs), implemented in parallel with resistors, as the basic circuit units. Although these JJs offer robust noise resistance and circuit stability, they occupy a large area, limiting the JJ process integration density to generally below 10^6 JJs/cm^2 [13]. To increase the integration scale of SFQ circuits beyond 10^6 JJs/cm^2, it is necessary to reduce the area occupied by JJs and shunt resistors. Unshunted JJs significantly reduce the unit area; therefore, they have become potential candidates for superconducting Josephson circuits requiring high integration density, high current density, and high clock frequencies [13].

Check for updates

Academic Editor: Costas Psychalinos

Received: 11 September 2026
Revised: 16 October 2026
Accepted: 21 October 2026
Published: 24 October 2026

Copyright: © 2026 by the authors. Licensee MDPI, Basel, Switzerland. This article is an open access article distributed under the terms and conditions of the Creative Commons Attribution (CC BY) license.

Compared to shunted JJs, unshunted JJs are more sensitive to electromagnetic and magnetic noise from circuits, space, and other sources. As a critical physical parameter of JJs, the critical current (I_c) is crucial for subsequent device and circuit design, as well as process preparation [14]. The accuracy of the I_c measurement directly affects the margins of various electrical parameters in subsequent circuits. To obtain accurate measurements, testing should ideally be conducted in a suitable shielding room [15]. However, due to laboratory constraints, actual tests are usually performed in unshielded environments. This inevitably introduces various environmental noises to the JJ, creating significant uncertainty in the measurement results of the JJ current. Furthermore, future superconducting computers will operate in noisy environments to remain competitive with semiconductor computers. Therefore, it is necessary to conduct accurate measurement research on unshunted JJ current in unshielded environments and evaluate filtering techniques applicable to such conditions.

According to the Ambegaokar–Baratoff theory [16], the theoretical value I_{c0} can be calculated using the formula $I_{c0} = I_g \times \pi/4$. Here, I_g is defined as the current at which the junction transitions to a normal state, and V_g is the gap voltage of the Josephson junction. The actually measured I_c value is usually smaller than the theoretical value I_{c0} due to complex noise effects, which seriously affect the circuit performance of superconducting Josephson devices. Yasushi Ishikawa et al. analyzed the influence of magnetic noise on the characteristics of superconductor/normal-metal/superconductor (SNS) JJ I_c and found that the dependence of Josephson currents on the magnetic field is sensitive to the width of the normal metal [17]. Ohkubo et al. [18] studied the standard measurement method of I_c in the over-damped regime; however, such studies for under-damped Nb/Al-AlO_x/Nb junctions under unshielded conditions are lacking.

In this paper, the influence of electromagnetic, magnetic, and flux noises on the accurate measurement of JJ I_c is experimentally studied based on unshunted JJs in an unshielded environment. This study provides a reference for avoiding or reducing the impact of the test environment and magnetic flux noise on I_c under actual experimental conditions. It has guiding significance and application value for the subsequent research and application of RSFQ circuits and superconducting large-scale digital integrated circuits.

2. Results and Discussion

2.1. JJ Fabrication Process and I_c Test Equipment

Comprehensive and efficient process control monitors (PCMs) are essential for maintaining the stability of physical parameters in Josephson junctions (JJs). Measurements were performed on an unshunted Nb/Al-AlOx/Nb JJ sample, designated SIMIT Nb03, fabricated using a standard process for RSFQ integrated circuits [19,20]. Given that junction quality is influenced by Nb film stress [20,21], JJs were designed on both a flat SiO_2 field and via a Mo resistor. The PCM includes two types of JJs: unshunted junctions on SiO_2 fields (labeled juf) and those on Mo resistors (labeled jur). The Mo and SiO_2 film thicknesses are 40 nm and 100 nm, respectively. Nb was patterned and etched using inductively coupled plasma reactive ion etching (ICP-RIE) with an endpoint detector. SiO_2 was deposited via plasma-enhanced chemical vapor deposition (PECVD) and etched by reactive ion etching (RIE) [22]. The sample identifier is s0506-juf3.1; the chip dimensions are 5 mm × 5 mm; and testing was conducted in a liquid helium environment.

The test circuit diagram is shown in Figure 1. The JJ was submerged 10 cm below the liquid helium surface to ensure it remained in a superconducting state during *I–V* curve measurements. Four π-type low-pass filter (LPF) units were integrated into the circuit to suppress environmental electromagnetic (EM) noise. In typical test environments, spatial EM noise at various frequencies, including power frequency (50 Hz) and RF signals (30 kHz–30 GHz), couples into the circuit as conductive noise, thereby affecting JJ

current measurements. Consequently, filtering circuits are necessary to mitigate these interference effects.

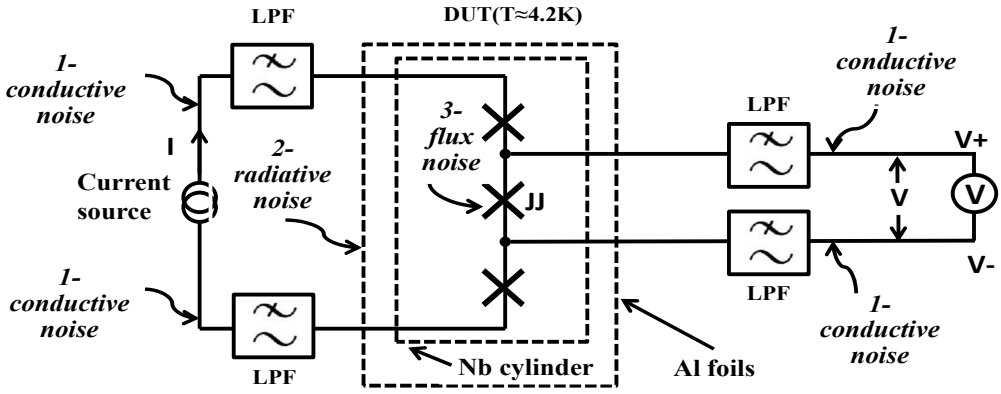


Figure 1. Schematic of the JJ device test circuit.

The I_c measurement setup is shown in Figure 2. A Keithley 6221 current source and a Keithley 2182A voltmeter(tektronix, Inc.US, Beaverton, OR, USA) were used to measure the *I-V* curve, from which the I_c value was automatically derived. The tested PCM cell was connected to the PCB via wire bonding. Ten layers of Al foil were wrapped around the Nb cylinder to shield against magnetic noise. Once the sample temperature cooled to ~4.3 K, the supply current amplitude was adjusted to twice the estimated maximum I_c, and the *I–V* curve was scanned and recorded by a computer. The maximum I_c is typically known from preceding current–voltage characteristic measurements. The entire experiment was controlled by a PC, with a current scanning step size of 4 μA. Further details on the testing procedure are available in our previous paper [11]. During testing, the sample was maintained below 10 cm of the liquid helium level. The de-fluxing process described herein involves: (1) raising the test rod to increase the sample temperature; (2) rotating the test rod by 90°, which may enhance the I_c value by mitigating directional magnetic field differences; and (3) maintaining the sample above 15 K for 5 min. Experimental results indicate that heating the sample to 15 K (compared to 10, 11, or 12 K for 10 s each) yields the highest I_c value. Finally, (4) the test rod is lowered to its original position for testing.

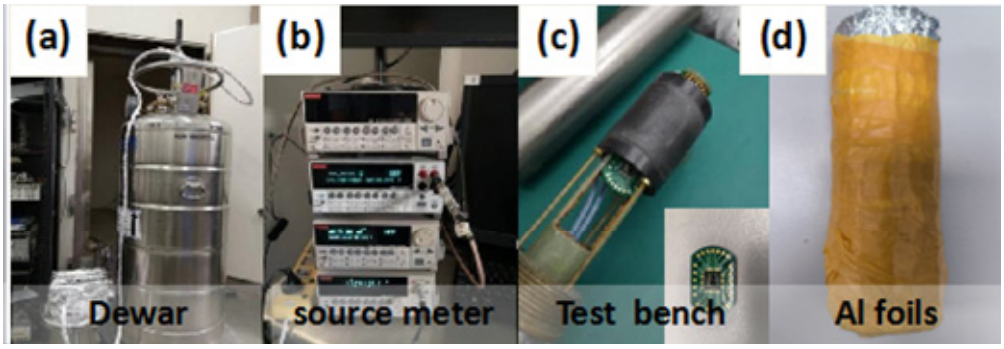


Figure 2. I_c measurement setup: (**a**) test bar in Dewar; (**b**) current source and voltmeter; (**c**) test bench; (**d**) Al foils.

Figure 3a presents the relationship between the measured and simulated normalized output amplitudes of the filter versus frequency, while Figure 3b shows a photograph of the filter PCB. The equivalent circuit diagram of the low-pass filter is illustrated in Figure 3b. The simulated curve represents the transfer function of a first-order Butterworth filter. The cut-off frequency is determined in Figure 3a at the point where the function value is 0.707. A comparison of the experimental and simulation data for Gfilter (f_c = 50 Hz) reveals

good agreement below 90 Hz. However, above 90 Hz, the experimental data gradually exceeds the simulation values. Similarly, in the Wfilter (f_c = 2 kHz) test, the experimental data exceeds the simulation data above 4 kHz. This discrepancy may be attributed to frequency-dependent noise interference above the cut-off frequency. To ensure effective filtering, a filter with an f_c (R = 5.1 kOhm, C = 10 F) of 5 Hz was employed in this study.

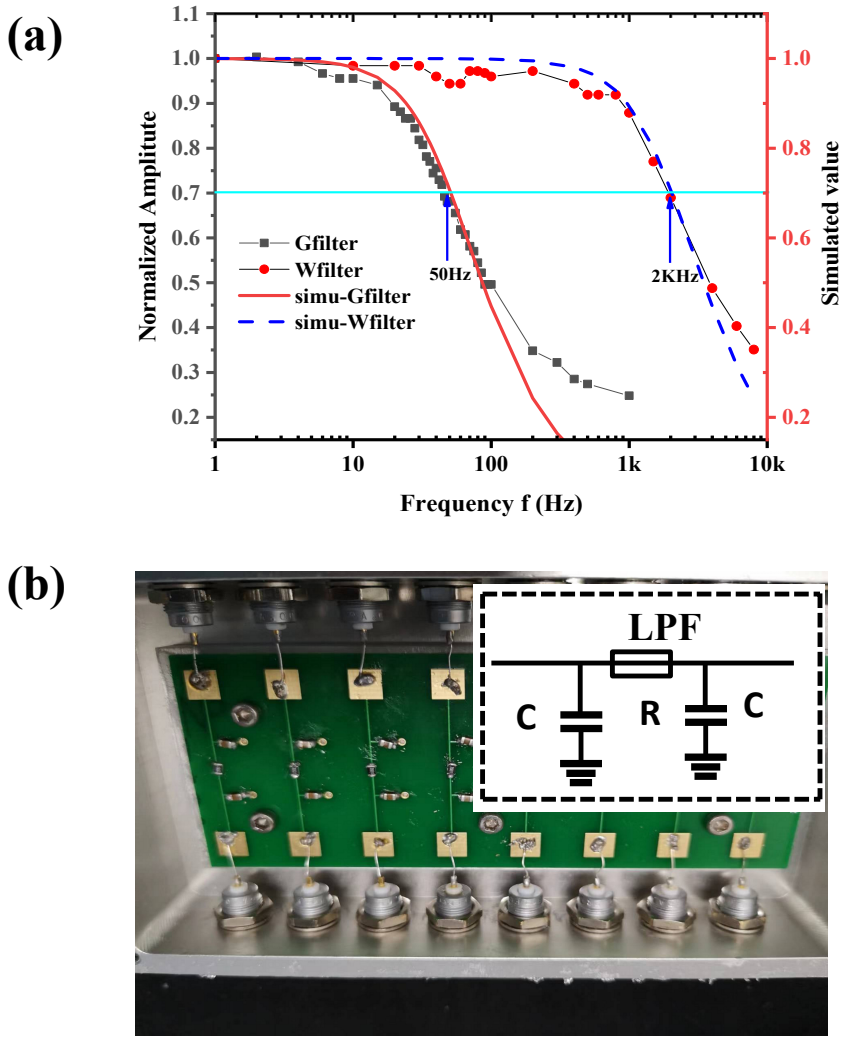


Figure 3. (**a**) Relationship between the measured (hexagons: 2 kHz; squares: 50 Hz) and simulated (solid line: 50 Hz; dotted line: 2 kHz) normalized output amplitude of the filter and frequency. The cut frequency is determined by the blue line. (**b**) Photograph of the filter PCB used for testing. Inset: Equivalent circuit diagram of the low-pass filter.

2.2. Definition of Physical Parameters Related to the Measurement of I_c

The schematic *I–V* curve is shown in Figure 4. The reciprocals of the slopes of L1, L2, and L3 correspond to the normal state resistance R_N, semi-superconducting state resistance R_s, and sub-gap resistance R_{sg}, respectively. I_g is defined as the vertical coordinate of the intersection (point N) of L1 and L2. I_M (=V_M/R_s) is defined as the vertical coordinate of the intersection (point M) of L2 and L3. The gap voltage V_g of the JJ is defined as 2Δ/e, where e is the electron charge and Δ is the superconducting energy gap [23]. L2 shares the same slope as the –V curve in the region R_sI_M V R_NI_g. R_N is the differential resistance dV/dI when $V > I_gR_N$. In this study, R_{sg} is the differential resistance dV/dI when V 2 mV. V_g is calculated using the formula V_g = 0.5 * (V_N + V_S) on line L2, where I is approximately 0.5 I_g.

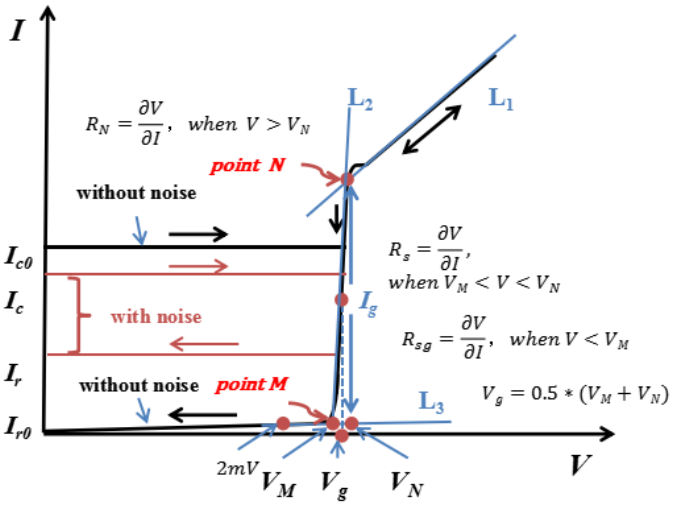


Figure 4. Schematic of the *I*–*V* curve.

In an ideal environment, the measured I_c approaches the ideal critical current I_{c0}, and the zero-voltage hysteresis current I_r approaches zero at 0 K. As I increases from 0 to I_{c0}, the voltage remains zero; when $I \geq I_{c0}$, V increases rapidly to V_g. When $I > I_g$ (quasi-particle current), the JJ enters the normal state with resistance R_N. In practical tests, magnetic and electromagnetic noise may introduce flux into the JJ sample, thereby decreasing I_c and increasing I_r.

3. Discussion

3.1. Effect of the Low-Pass Filter with Cut-Off Frequency f_c on I_c

The I_c measurements for sample s0506-juf3.1, repeated 30 times for each filtering configuration outside the magnetic shield room, are shown in Figure 5. The average I_c without a filter (upward triangle) is significantly lower than that with filters, indicating that filtering is necessary to suppress conductive noise along the cables and ensure higher I_c values. The bulge in the I_c curve for the unfiltered case may be caused by the sudden disappearance of surrounding noise, which induces an increase in I_c. The I_c values without a filter appear almost constant after 22 measurements compared to those before the 21st measurement, which may be attributed to flux trapping in the unshielded environment.

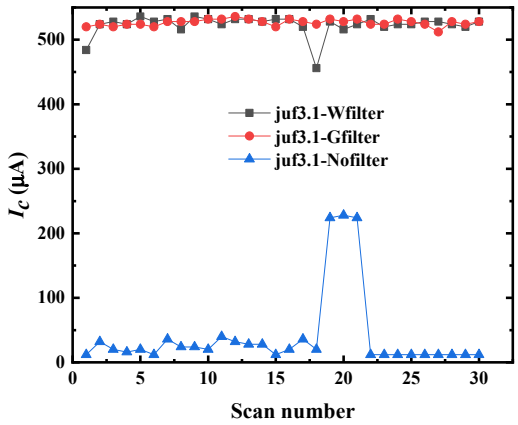


Figure 5. I_c data of sample s0506-juf3.1 from repeatability study. Gfilter: f_c = 50 Hz; Wfilter: f_c = 2 kHz.

The histograms of I_c for sample s0506-juf3.1 using different filters with different cut-off frequencies are shown in Figure 6. Comparing the two curves with filter cut-off frequencies

f_c of 50 Hz (Gfilter, Figure 6b) and 2 kHz (Wfilter, Figure 6a) reveals that the average I_c is nearly identical (~520 μA). However, the I_c obtained with the lower cut-off frequency (f_c = 50 Hz) exhibits better I_c uncertainty than that with the higher f_c (2 kHz). This indicates that a filter with a lower cut-off frequency is preferable for achieving both good uncertainty and high average I_c. Electromagnetic noise, such as power frequency interference, can be filtered out by a filter with a cut-off frequency lower than 50 Hz, thereby improving the measured I_c value and reducing uncertainty.

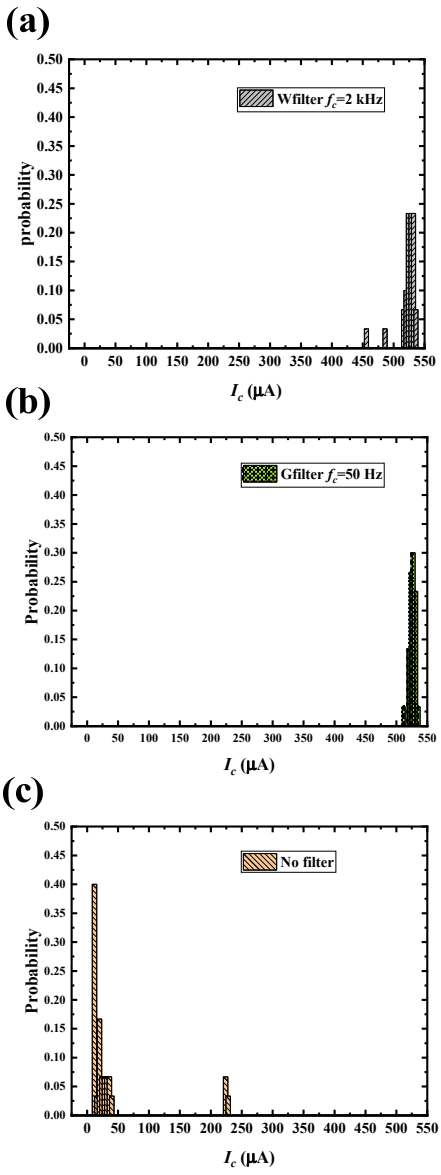


Figure 6. Histogram of I_c data for sample s0506-juf3.1 from the repeatability study. The filter types and cut-off frequencies are as follows: (**a**) Wfilter: f_c = 2 kHz; (**b**) Gfilter: f_c = 50 Hz; (**c**) No filter.

3.2. Effect of the Nb Cylinder and Multi-Layer Al Foils on the Measured I_c Value

Magnetic fields, flux vortices, and electromagnetic interference can penetrate superconducting films and devices through various mechanisms, leading to uncertainty in I_c measurements and ultimately affecting circuit operation. Therefore, shielding is necessary during measurements to mitigate these effects.

The I_c measurements for sample s0506-juf3.1, repeated 41 times with and without an Al cover, are shown in Figure 7a. The probability distributions of I_c with and without Al foils are presented in Figure 7b. The shielding structure consists of a Nb cylinder surrounded by

10 layers of Al foil. The average I_c and uncertainty with the cover are 349 μA and ±11%, respectively, whereas those without the cover are 299 μA and ±11%, respectively.

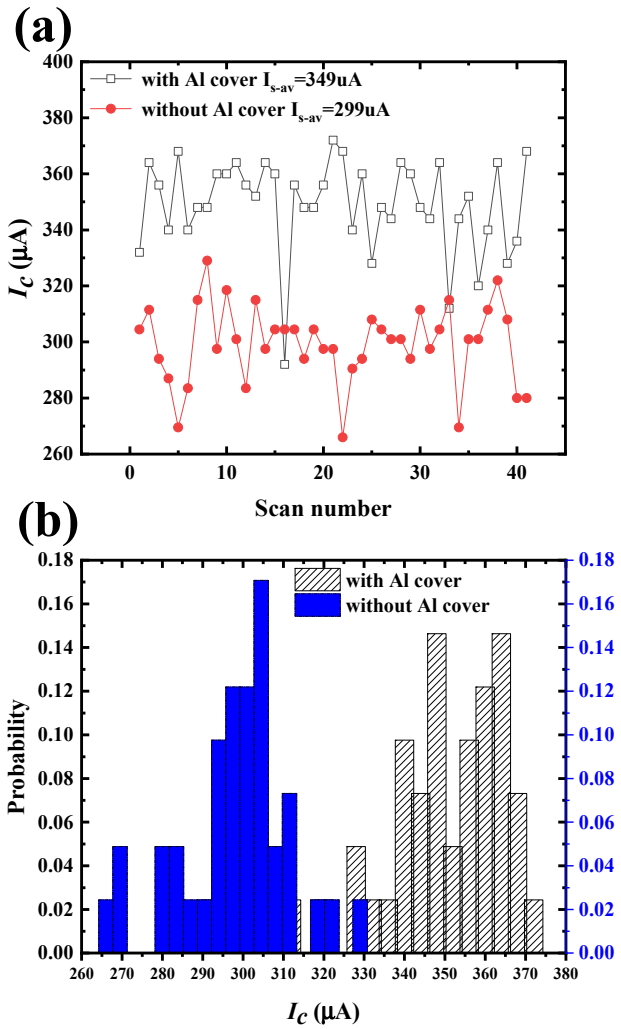


Figure 7. (**a**) I_c data for sample s0506-juf3.1 from the repeatability study, measured with (blank squares) or without (full circles) Al foil; (**b**) Histogram of the same data with (black diagonal bars) and without (blue blank bars) Al foil.

3.3. Influence of Multiple De-Fluxing on I_c with and Without Spatial EM and Magnetic Noise

The I_c repeatability for different de-fluxing durations is presented in Figure 8a, while the histogram of the same data is shown in Figure 8b. It is evident that different de-fluxing times correspond to distinct average I_c values. Table 1 reports the uncertainty and average I_c for conditions including no de-fluxing, the first through fourth de-fluxing cycles outside the magnetic shield room, and measurements within the magnetic shield room (full shield). The average I_c after the second de-fluxing cycle is the lowest (102 μA), corresponding to the largest uncertainty. One reason for the deviation in I_c from the average I_c value outside the magnetic shield room is environmental electromagnetic (EM) noise, which may introduce flux into the sample and reduce I_c. In contrast to measurements outside the shielded room, the highest average I_c (560.13 μA) and lowest uncertainty (0.13%) were obtained within the magnetic shield room. The theoretical I_c (=I_g π/4) is calculated to be 668.82 μA.

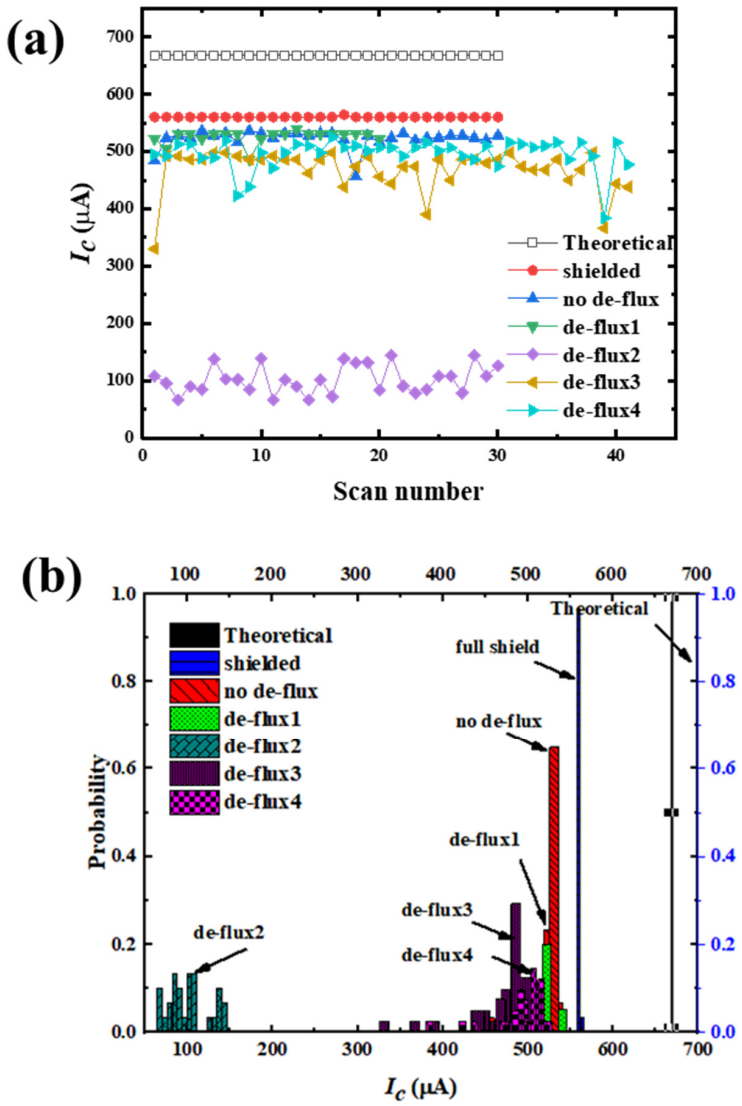


Figure 8. (**a**) I_c data of sample s0506-juf3.1 from the repeatability study, following several de-fluxing cycles; (**b**) histogram of the same data. Insets associate the curves with each de-fluxing cycle: theoretical data, data in full shield with no de-fluxing, and data after the first, second, third, and fourth de-fluxing cycles.

Table 1. The uncertainty and average value of I_c with no de-fluxing, after the 1st, 2nd, 3rd, and 4th de-fluxing cycles outside the magnetic shielding room, inside the shielding room, and with theoretical I_c.

Item	No De-Flux	De-Flux1	De-Flux2	De-Flux3	De-Flux4	Full Shield	Ideal
U (%)	3	2.25	24.18	7.59	5.44	0.13	0
I_c (μA)	523.07	526.05	102	469.02	495.95	560.1	668.8

3.4. Flux Noise Impact and Its Removal or Reduction

The I_c distributions for no de-fluxing, de-flux 1, de-flux 2, de-flux 3, and de-flux 4 are shown in Figure 8b. The peak position of the I_c distribution represents the most frequently measured I_c value. Different de-fluxing cycles exhibit different I_c peak values and distributions; notably, the first de-fluxing cycle shows the maximum I_c in Figure 8a, indicating that the I_c value is not positively correlated with the number of de-fluxing cycles. Using this method, the measured I_c value under EM and magnetic noise conditions reaches 526.05 μA, which is 93.9% of the value (560.13 μA) tested in the magnetic shielding room.

As shown in Table 1, the uncertainty U of the sample varies with the number of de-fluxing cycles, and the uncertainty in the fully shielded environment is lower than that of all other tested data under unshielded conditions. The data tested under the unshielded environment also vary significantly with de-fluxing times, but the uncertainty does not show a clear positive or negative correlation with the number of de-fluxing cycles. This may be explained by the fact that spatial magnetic fields and EM noise randomly affect the flux trapping mechanism in the tested sample under unshielded conditions, thereby causing the I_c uncertainty to fluctuate. Therefore, if test conditions permit, it is necessary to perform de-fluxing in a magnetically shielded environment to reduce uncertainty.

3.5. Discussion on Circuit Scattering Noise and Thermal Fluctuations

Circuit scattering noise satisfies the central limit theorem, resulting in a Gaussian distribution of jump statistics; conversely, thermal fluctuations and thermal escape yield jump statistics that follow a Lorentzian distribution. A significant number of additional counting points appear in the tails of the histogram for thermal noise, serving as an experimental criterion to distinguish between these two noise types.

Figure 6 presents the current measurement histograms under three different cut-off frequency conditions. The histogram for the circuit with a 50 Hz cut-off frequency closely approximates a Gaussian distribution, whereas the unfiltered measurement results exhibit a Lorentzian distribution. The histogram for the 2 kHz cut-off frequency lies between these two distributions. This indicates that filters with lower cut-off frequencies more effectively suppress circuit noise, thereby yielding higher average current measurements.

3.6. Impact of Magnetic Noise and Its Mitigation

This study demonstrates that magnetic shielding reduces the influence of magnetic noise on the measurement of the junction critical current I_c by wrapping 10 layers of Al foil around the Nb cylinder enclosing the sample. General principles of magnetic and electromagnetic shielding, including the design and calculation of shielding effectiveness, are detailed in standard textbooks [24–26]. Iwashita et al. proposed a passive magnetic shielding method based on a niobium/aluminum structure. Theoretical analysis proves that this structure, combining high-permeability and superconducting materials, not only overcomes the shielding limit imposed by the critical field of niobium (approximately 170 mT) but also optimizes the temperature gradient of the radial thermal conductive layer, thereby enhancing the magnetic flux exclusion effect in the sample [27]. Although no experimental report was provided in the cited work, our test data for Nb/Al-AlO_x/Nb samples reveal that the average I_c of the sample in the Nb cylinder wrapped with Al foil is 16.7% higher than that of the unwrapped sample (Figure 7). Experiments indicate that wrapping aluminum foil around the Nb cylinder reduces magnetic leakage and increases the probability of magnetic flux exclusion from the superconducting layer, consistent with Iwashita's theoretical predictions. Furthermore, the current measurement distribution with Al coating tends to follow a Gaussian distribution, whereas the distribution without Al coating tends to follow a Lorentzian distribution. This suggests that the Al coating mitigates the influence of thermal fluctuations on the measurements, resulting in a relatively higher average current.

3.7. An Empirical Formula for Predicting I_c Values in Shielded Environments from Unshielded Environment Data

Figure 9 illustrates the relationship between the average JJ current $I_{c\text{-}av}$ and the uncertainty U of the I_c data for sample s0506-juf3.1 obtained from the repeatability study.

Based on the test procedure, a formula is proposed for predicting the measured I_c value in a magnetically shielded environment.

$$I_{ci-av} = y_0 + A_1 \times \exp(-U/t_1) \quad (1)$$

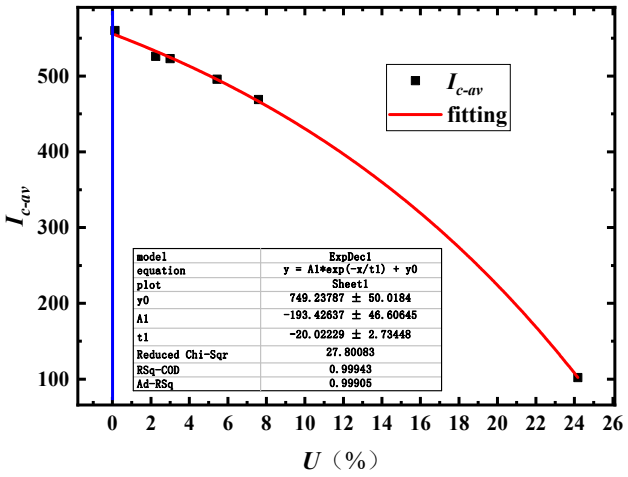


Figure 9. Relationship between the average JJ current $I_{c\text{-}av}$ and the uncertainty U of the I_c data for sample s0506-juf3.1 from the repeatability study. The red line represents the fitting curve; the red squares denote experimental data; and the blue vertical line indicates the condition where U equals 0.

The experimental procedure was as follows: (1) The sample was placed at the bottom of the testing rack; (2) the test rod was inserted into the liquid helium Dewar, maintaining the sample 10 cm below the liquid helium level during testing; (3) all devices were connected; (4) the system waited until the sample temperature dropped below 4.3 K; (5) I_{cij} (i = 1:n; j = 1:m) was measured. Specifically, I_{cij} was measured m times; if j < m, j was incremented by 1 and I_c was measured again; if j = m, the average value $I_{ci\text{-}av}$ and uncertainty U_i were obtained, and the sample was heated to de-flux. (6) n measurements of $I_{ci\text{-}av}$ were performed; if i < n, i was incremented by 1; if i = n, the process ended, outputting $I_{ci\text{-}av}$ and U_i. (7) The relationship between $I_{ci\text{-}av}$ and U_i was established using formula (1).

Fitting the data in Figure 9 yielded y_0 = 749 μA, A_1 = −193 μA, and t_1 = 20. Based on the relationship between $I_{ci\text{-}av}$ and U_i, the average I_{ci} was extrapolated to the point where U = 0, resulting in I_c = 556 μA. This value represents the empirical I_c under unshielded conditions. The experimentally measured I_c under shielded conditions was 560 μA. A deviation of less than 1% verifies the effectiveness of the empirical formula in predicting I_c values for sample s0506-juf3.1 in shielded environments using data from unshielded environments.

The s0506-juf2.8 sample was also measured, exhibiting a similar $I_{c\text{-}av}$ versus U relationship despite having only three data points. Specifically, a larger $I_{c\text{-}av}$ corresponded to smaller uncertainty, allowing the true value of $I_{c\text{-}av}$ at U = 0 to be obtained through fitting.

This empirical formula is applicable to sample s0506-juf3.1. Although measurements were attempted on other samples, the data were insufficient for verification. Therefore, further validation using data from additional systems will be conducted in future work.

4. Conclusions

The influence of magnetic and electromagnetic noise on the accurate measurement of the junction critical current I_c was investigated using unshunted Nb/Al-AlO_x/Nb JJ samples. Magnetic flux accumulation within the junction is the primary cause of the decrease in JJ I_c, whereas electromagnetic (EM) noise, as an external factor, mainly contributes to increased uncertainty and reduced I_c values. The specific findings are summarized as follows:

Experimental results demonstrate that magnetic flux pinning in the superconductor–insulator–superconductor (SIS) junction is a significant factor contributing to the reduction in the measured JJ current. Multiple de-fluxing procedures, involving changes in the rotation direction of the test rod before each cycle, facilitate the acquisition of higher I_c measured values. By performing repeated de-fluxing (more than five times) and selecting the optimal I_c value, the measured current reached 526.05 μA across 41 cycles, representing 93.9% of the value (560.13 μA) obtained in a shielded room. Furthermore, rotating the test rod by 90 degrees during the thermal cycle yielded a high average test current. Similar phenomena have been reported in reference [15].

The use of a Nb cylinder wrapped with multi-layer aluminum foil effectively reduces magnetic interference. This configuration increased the JJ I_c value by 16.7%.

An empirical formula was established to predict I_c values in shielded environments based on data from unshielded conditions. The deviation between the empirical I_c predictions and the experimentally measured values was less than 1%, thereby verifying the effectiveness of the proposed formula.

This study presents a relatively accurate and low-cost method for testing JJ I_c under unshielded conditions. This approach provides guidance for precise I_c measurements in conventional laboratories without expensive magnetic shielding equipment, offering significant practical value for accelerating the design and manufacturing of RSFQ devices and large-scale superconducting computer-integrated circuit chips.

5. Patents

The low-temperature superconducting Josephson junction current testing method without magnetic shielding environment and parallel resistance is attributed to Zhou Jian, Wang Juan, Wang Yongliang, and Peng Wei. Invention patent: application number: 202311206205.0; application date: 19 September 2023 Accepted. Authorization number: ZL202311206205.0; authorization date: 4 August 2026.

Author Contributions: Conceptualization, J.Z.; investigation, J.Z.; resources, Y.Y. and J.W.; writing—original draft preparation, J.Z.; writing—review and editing, Y.W.; supervision, W.P. and M.W. All authors have read and agreed to the published version of the manuscript.

Funding: This research was supported by the Strategic Priority Research Program of Chinese Academy of Sciences under Grant XDA18000000.

Data Availability Statement: All experimental data presented in this study are included in the article. Additional inquiries can be directed to the corresponding author.

Conflicts of Interest: The authors declare no conflicts of interest.

Abbreviations

The following abbreviations are used in this manuscript:

JJ	Josephson junction
RSFQ	Superconducting rapid single flux quantum
PCMs	Process control monitors
PECVD	Plasma-enhanced chemical vapor deposition

References

1. Chen, W.; Rylyakov, A.V.; Patel, V.; Lukens, J.E.; Likharev, K.K. Superconductor digital frequency divider operating up to 750 GHz. *Appl. Phys. Lett.* **1998**, *73*, 2817–2819. [CrossRef]
2. Ren, J.; Semenov, V.K. Progress with physically and logically reversible superconducting digital circuits. *IEEE Trans. Appl. Supercond.* **2011**, *21*, 780–786. [CrossRef]

3. Tolpygo, S.K. Superconductor digital electronics: Scalability and energy efficiency issues (Review Article). *Low Tem. Phys.* **2016**, *42*, 361–379. [CrossRef]
4. Tolpygo, S.K.; Bolkhovsky, V.; Weir, T.J.; Johnson, L.M.; Gouker, M.A.; Oliver, W.D. Fabrication process and properties of fully-planarized deep-submicron Nb/Al-AlOx/Nb Josephson junctions for VLSI circuits. *IEEE Trans. Appl. Supercond.* **2015**, *25*, 1101312. [CrossRef]
5. Tolpygo, S.K.; Bolkhovsky, V.; Weir, T.; Wynn, A.; Oates, D.; Johnson, L.; Gouker, M.A. Advanced fabrication processes for superconducting very large scale integrated circuits. *IEEE Trans. Appl. Supercond.* **2016**, *26*, 1100110. [CrossRef]
6. Li, F.; Peng, W. Research status and prospects of cryogenic storage for superconductor digital computing. *J. Funct. Mater. Devices* **2026**. [CrossRef]
7. Yang, S.C.; Chen, M.F.; Ren, J. Time scaling methodology for superconducting dual-active-layer integrated circuits. *J. Funct. Mater. Devices* **2026**, *32*, 032205. [CrossRef]
8. Manheimer, M.A. Cryogenic computing complexity program: Phase I introduction. *IEEE Trans. Appl. Supercond.* **2015**, *25*, 1301704. [CrossRef]
9. Yang, S.C.; Ren, J.; Gao, X.P.; Gao, Y.T.; Lin, Y.X.; Wang, M.E.; Zhao, W.B. Design automation systems for rapid single flux quantum logic. *IEEE Trans. Appl. Supercond.* **2026**, *36*, 1301105. [CrossRef]
10. Wang, S.M.; Gao, X.; Ren, J. RCLSJ model correction and verification by a proposed test method for DFF's high-frequency performance. *Supercond. Sci. Technol.* **2025**, *38*, 055011. [CrossRef]
11. Gao, X.P.; Feng, Y.X.; Niu, M.H.; Gao, X.; Liu, H.L.; Weng, B.C.; Yang, S.C.; Zhang, X.; Ying, L.L.; Zhao, W.B.; et al. A 4-Nb-layer cell library suitable for LSI superconductor digital circuits. *IEEE Trans. Appl. Supercond.* **2025**, *35*, 0600405. [CrossRef]
12. Gao, X.; Liu, H.L.; Gao, X.P.; Zhang, X.; Ren, J. Timing evaluation of passive transmission line by RSFQ ring oscillator. *IEEE Trans. Appl. Supercond.* **2024**, *34*, 1300605. [CrossRef]
13. Tolpygo, S.K.; Bolkhovsky, V.; Zarr, S.; Weir, T.J.; Wynn, A.; Day, A.L.; Johnson, L.M.; Gouker, M.A. Properties of unshunted and resistively shunted Nb/AlOx-Al/Nb Josephson junctions with critical current densities from 0.1 to 1 mA/μm2. *IEEE Trans. Appl. Supercond.* **2017**, *27*, 2667403. [CrossRef]
14. West, J.T.; Kurlej, A.; Wynn, A.; Rogers, C.; Gouker, M.A.; Tolpygo, S.K. Wafer-scale characterization of a superconductor integrated circuit fabrication process using a cryogenic wafer prober. *IEEE Trans. Appl. Supercond.* **2022**, *32*, 3172660. [CrossRef]
15. Zhou, J.; Wang, J.; Yao, Y.W.; Wang, Y.L.; Wang, M.; Peng, W. A measurement method of critical current of unshunted Josephson junctions. *IEEE Trans. Appl. Supercond.* **2023**, *33*, 1–6. [CrossRef]
16. Ambegaokar, V.; Baratoff, A. Tunneling between superconductors. *Phys. Rev. Lett.* **1963**, *10*, 486–489. [CrossRef]
17. Ishikawa, Y.; Fukuyama, H. Effects of magnetic field on Josephson current in SNS system. *J. Phys. Soc. Jpn.* **1999**, *68*, 954–963. [CrossRef]
18. Ohkubo, M.; Uehara, G.; Beyer, J.; Mimura, M.; Tanaka, H.; Ehara, K.; Tanaka, S.; Noguchi, T.; Mitchell, E.E.; Foley, C.P.; et al. Standard measurement method for normal state resistance and critical current of resistively shunted Josephson junction. *Supercond. Sci. Technol.* **2022**, *35*, 045002. [CrossRef]
19. Zhang, X.; Ying, L.; Niu, M.; Zhang, H.; Liu, H.; Wu, Y.; Xu, W.; Chen, L.; Shao, Y.; Liang, T.; et al. Process control monitoring for fabrication technology of superconducting integrated circuits. *IEEE Trans. Appl. Supercond.* **2021**, *31*, 1101206. [CrossRef]
20. Ying, L.L.; Zhang, X.; Niu, M.; Ren, J.; Peng, W.; Maezawa, M.; Wang, Z. Development of multi-layer fabrication process for SFQ large scale integrated digital circuits. *IEEE Trans. Appl. Supercond.* **2021**, *31*, 3065277. [CrossRef]
21. Satoh, T.; Hinode, K.; Akaike, H.; Nagasawa, S.; Kitagawa, Y.; Hidaka, M. Fabrication process of planarized multi-layer Nb integrated circuit. *IEEE Trans. Appl. Supercond.* **2005**, *15*, 78–81. [CrossRef]
22. Wu, Y.; Ying, L.; Li, G.; Zhang, X.; Peng, W.; Ren, J.; Wang, Z. Film stress influence on Nb/Al-AlOx/Nb Josephson junctions. *IEEE Trans. Appl. Supercond.* **2019**, *29*, 1102105. [CrossRef]
23. Alam, S.; Jahangir, M.A.; Aziz, A. A compact model for superconductor-insulator-superconductor (SIS) Josephson junctions. *IEEE Electron Device Lett.* **2020**, *41*, 1249–1252. [CrossRef]
24. Rikitake, T. *Magnetic and Electromagnetic Shielding*; Springer Science & Business Media, Kluwer: Berlin/Heidelberg, Germany, 1987.
25. Celozzi, S.; Araneo, R.; Lovat, G. *Electromagnetic Shielding*; IEEE Press and Wiley Interscience (Wiley): Hoboken, NJ, USA, 2008.
26. Braginski, A.I. Superconductor electronics: Status and outlook. *J. Supercond. Nov. Magn.* **2019**, *32*, 23–44. [CrossRef]
27. Iwashita, Y.; Kuriyama, Y.; Tongu, H.; Fuwa, Y. Magnetic field shielding with superconductors. *IEEE Trans. Appl. Supercond.* **2022**, *32*, 3500404. [CrossRef]

Disclaimer/Publisher's Note: The statements, opinions and data contained in all publications are solely those of the individual author(s) and contributor(s) and not of MDPI and/or the editor(s). MDPI and/or the editor(s) disclaim responsibility for any injury to people or property resulting from any ideas, methods, instructions or products referred to in the content.